Silsesquioxane−Urethane Hybrid for Thin Film Applications

Matthew Oaten and Namita Roy Choudhury*

ARC Special Research Centre for Particle and Material Interfaces, Ian Wark Research Institute, University of South Australia, Mawson Lakes, South Australia, Australia

Received November 14, 2004; Revised Manuscript Received May 13, 2005

ABSTRACT: Transparent polyurethane hybrid containing an inorganic open cage polyhedral oligomeric silsesquioxane was synthesized for thin film applications. The resulting material was characterized using various spectroscopic, microscopic, thermal, and scattering techniques. Modulated differential scanning calorimetry (MDSC) in conjunction with photoacoustic Fourier transform infrared spectroscopy (PA-FTIR) has enabled to probe the reaction and chemical structure of the hybrid. ^{29}Si solid-state nuclear magnetic resonance spectroscopy results prove the formation of the urethane hybrid. The evolution of the hybrid structure during the reaction was investigated using small-angle neutron scattering (SANS). The coating, when applied to clean steel substrates via dip coating, reveals a uniform, dense, and essentially defect-free morphology. Analysis by angle-resolved X-ray photoelectron spectroscopy (XPS) has allowed the interface between the substrate and the coating to be probed. It is found that the POSS−urethane coating forms a lamellar structure rather than a random 3D network.

Introduction

Thin film coatings on metallic components are routinely employed for a wide variety of purposes, including protection from environmental and abrasive attack, antifriction requirements, and aesthetic considerations. It is common for metallic components to be protected by ceramic coatings, although several other types of substrate/coating combinations are also routinely employed. Various organic coatings such as polyimides, polyurethanes, polyesters, polyacrylates, and polystyrenes are known to perform well in corrosion and/or abrasion tests, and combinations of different polymer species allow the tailoring of properties such as thermal stability and electrical impedance. However, there are shortcomings in using organic polymers because of the following features: (a) they have hydrophilic characteristics; (b) microorganisms readily settle and grow on them, leading to degradation; (c) they display poor wetting and adhesive properties to metals; and finally (d) they often form mechanically weak films.[1] Thus, there is a distinct need to develop superior materials that can overcome these problems.

In recent years, polyhedral oligomeric silsesquioxane (POSS)-based hybrid polymers have emerged as unique materials for various applications.[2−6] The growing interest in these POSS hybrids stems from their characteristic architectural features, which offer the end products' enhanced properties as compared to alternative hybrid polymer systems. Silsesquioxanes bearing reactive functionalities can be reacted with organic precursors to create hybrids with well-ordered structures and excellent properties. These properties, for example, include adhesion to various substrates, abrasion resistance, flexibility, toughness, and excellent resistance to chemicals, solvents, and water.[3,4] Thus, the potential of hybrid-based coating systems is apparent. Conventional polyurethanes find extensive use as protective coatings. However, they are known to exhibit poor resistance to heat; e.g., the acceptable mechanical properties (strength, moduli, etc.) generally disappear above 80−90 °C, and thus their application in exposed conditions is limited.[5] The ability to design coatings from the molecular level up represents the significant potential to develop multifunctional coatings. A potentially viable method to improve the thermal stability of polyurethane systems is by the incorporation of highly thermally stable POSS moieties to produce hybrids with high glass transition temperature (T_g) and remarkable chemical, mechanical, and thermal stability. Because their rigid framework closely resembles that of silica, silsesquioxanes can form hard, abrasion-resistant coatings with high thermal stability.

POSS molecules have been successfully incorporated into many traditionally pure organic systems, such as epoxies,[2−4] imides,[5] methacrylates,[6] and rubber compounds.[7,8] The unique architecture and variety of POSS chemicals available are generally incorporated into chemical systems in a number of ways. POSS hybrids can be produced by covalently bonding POSS groups into a polymer chain, or they may be attached to polymer chains as pendant molecules. Alternatively, they may be blended with a polymer matrix. Not surprisingly, significant property enhancements have been reported for some of these POSS hybrid systems, including increased toughness, decreased flammability, high ultraviolet stability, and increased oxidation resistance.

There are only a few investigations into urethanes containing POSS systems. Recently, Neumann et al.[9] synthesized a POSS−urethane hybrid utilizing poly(ethylene glycol) and an octakis(dimethylsiloxy)octasilsesquioxane ($Q_8M_8^H$) core functionalized with eight isocyanate groups—termed $Q_8M_8^{TMI}$. The POSS-based elastomer showed thermal stability up to 190 °C. In other studies, Fu et al.[10] and Hsiao et al.[11] produced a polyurethane elastomer with POSS groups pendant to the polymer chain. The effect of the POSS groups acting as molecular reinforcers in the hard segment enhanced the microphase separation between the hard and soft segments and was shown to greatly improve the tensile modulus and strength, as compared to the same urethane without the POSS molecules. Recently, Wilkes et

* Corresponding author: Ph 61 8 8302 3719; Fax 61 8 8302 3755; e-mail Namita.Choudhury@unisa.edu.au.

10.1021/ma0476543 CCC: $30.25
Published on Web 06/28/2005

al.[12] explored the potential of POSS and spherosilicate containing hybrids for abrasion-resistant coatings. However, to date, to our knowledge, there is no evidence in the literature on POSS−urethane materials intended for use as protective thin films.

In this work, we have utilized an open-caged POSS structure containing three functional hydroxyl groups and an aliphatic diisocyanate species to produce a urethane with a POSS core in the polymer chain, with the ultimate aim of fabricating a hard, abrasion- and corrosion-resistant, barrier thin film coating for metals.

Experimental Section

Materials. Hexamethylene diisocyanate and dibutyl tin dilaurate catalyst were purchased from Aldrich, Australia, and used as received. Trisilanol isobutyl POSS ($Si_7O_{10}C_{28}H_{66}$), henceforth referred as T-POSS, was purchased from Hybrid Plastics and used as received. Toluene purchased from ACE Chemicals, Australia, was used after distillation followed by refluxing over sodium metal with benzophenone until a dark blue color was obtained from the benzophenone ketyl radical.

Synthesis of the T-POSS−Urethane Hybrid. The T-POSS−urethane hybrid was synthesized by the reaction of hexamethylene diisocyanate (HDI) and trisilanol isobutyl POSS at a stoichiometric molar ratio of 2:1 (T-POSS:HDI). Dibutyl tin dilaurate (DBTL) was used as the catalyst. A solution of HDI (0.1065 g, 0.000633 mol) in dry toluene (15 mL) was added dropwise to a mixture of T-POSS (1.0023 g, 0.00126 mol) and the DBTL catalyst (20 μL) in dry toluene (40 mL) under nitrogen in a dry three-necked, round-bottom flask fitted with a condenser and a magnetic stirrer. The reaction flask was immersed in an oil bath at 60 °C. The reaction progress was monitored via transmission FTIR, and the reaction was deemed complete when the isocyanate band at 2268 cm^{-1} had disappeared completely. The reaction was complete in 4 h. Such a molar ratio of the reactants allows the formation of a polyurethane hybrid, which can form a cross-linked network via condensation of the free silanol groups, as confirmed by PA-FTIR and MDSC. The network formation is physically complemented by the presence of hydrogen bonding between urethane groups.

The hybrid coating was applied to steel substrates via the following procedure: cold rolled steel was ultrasonically solvent cleaned to remove surface oils; this was followed by immersion in a commercial alkaline cleaner at 80 °C for 5 min. The purpose of the alkaline treatment was to produce a fresh oxide layer for chemical bonding to the hydroxyl groups of the hybrid urethane. Confirmation of the formation of the oxide layer was achieved by XPS. This method of surface preparation has been well documented by various authors.[13−18] The prepared steel substrate was then dip-coated into a 1% m/v T-POSS−urethane hybrid solution in dry toluene for 1 min and then blown with compressed air to remove the excess coating solution. The coated sample was placed in an oven at 80 °C in air for 1 week for curing. The evaporation of remaining solvent followed by matrix cross-linking resulted in an optically transparent film. The coated sample was then subjected to solvent rinsing to remove any physisorbed layers.

1. Characterization of the Hybrid and Thin Film on Metal. a. Spectroscopic Characterization. Solid-State ^{29}Si NMR. Solid-state ^{29}Si NMR was performed using MSL 300 MHz (Bruker) instrument to evaluate the structure of the hybrid. Cross-polarization and magic-angle spinning (CP/MAS) were used to obtain the spectra. The spinning rate was 4 kHz. A radio frequency of 62.5 kHz was used for cross-polarization and proton decoupling (90° pulse width for ^{1}H = 4 μs). A standard Bruker 4 mm CPMAS probe was used. Recycle delay time was 20 s.

b. Small-Angle Neutron Scattering Analysis (SANS). Analysis via SANS of the T-POSS−urethane reaction was carried out to study the in-situ formation of the hybrid at a temperature of 60 °C and using deuterated toluene as the solvent. The SANS experiments were performed with the small-angle neutron diffractometer at the Bragg Institute, Australian Nuclear Science and Technology Organisation (ANSTO), located at Lucas Heights, Sydney, using the AUSANS instrument. The neutron wavelength λ was 3.5 Å with a dispersion of $\Delta\lambda/\lambda$ of 0.01. The sample-to-detector distance was fixed at 5 m. The Q range of the instrument was 0.01−0.1 (scattering vector, $q = [4\pi/\lambda] \sin(\theta/2)$). The sample temperature was controlled to within ±0.5 °C using a circulating bath. The two-dimensional scattering data were circularly averaged to produce one-dimensional scattering intensity $I(Q)$ vs Q. The data were corrected for background, pure solvent, and scattering contribution from the empty cell and normalized to constant beam intensity. The measurements were made using quartz cells. Additionally, the data were adjusted for detector sensitivity and placed on an absolute intensity scale using a calibrated silica standard sample (Sil A2) provided by ANSTO.

c. Photoacoustic Fourier Transform Infrared Spectroscopy (PA-FTIR). IR spectra of the synthesized T-POSS−urethane and residue samples from the thermal analysis experiments were recorded between 4000 and 400 cm^{-1}, with a resolution of 4 cm^{-1} and 512 scans in a helium atmosphere on a Nicolet Magna spectrometer (model 750) equipped with a MTEC (model 300) photoacoustic cell. Samples were purged with helium at a flow rate of 10 cm^3/min for several minutes before spectra were recorded. Helium was chosen as the purge gas due to its high thermal conductivity. Carbon black was used as the reference material.

d. Angle-Resolved X-ray Photoelectron Spectroscopy (AR-XPS). Depth profiling of the T-POSS−urethane coating on a steel substrate was performed with a Physical Electronics PHI 5600 ESCA system fitted with a Mg Kα anode (λ = 1253.6 eV). XPS spectra were acquired at takeoff angles of 15°, 30°, 45°, 60°, and 90° with a pass energy of 23.5 eV. Charge correction was performed by fixing the hydrocarbon component of the C 1s peak to 284.6 eV.

2. Thermal Analysis. Thermogravimetric analysis (TGA) was carried out using a TA Instruments TGA 2950 in the temperature range of 30−600 °C at a heating rate of 10 °C/min under a nitrogen atmosphere. The mass of sample used was between 10 and 12 mg. The onset of degradation, the weight loss due to different components, and the residue remaining were evaluated. The temperature at which the rate of mass loss (T_{max}) is maximum was evaluated from the differential thermogravimetry (DTG) curves.

Modulated differential scanning calorimetry (MDSC) was carried out on a TA Instruments DSC Q100 series with a heating rate of 2 °C/min under a nitrogen atmosphere. The sample mass was ≈8 mg. Modulation conditions of ±0.42 °C every 80 s were used. The unit was fitted with a refrigerated cooling system (RCS).

Thermal cycling of the T-POSS−urethane sample was carried out using the Q100 model. A 20 mg sample of the hybrid was cycled for a total of four times through a temperature range of −80 to 250 °C at 5 °C/min.

3. Microscopic Characterization. Atomic force microscopy (AFM) was performed in pulsed force mode (PFM)[19,20] in which the mapping of surfaces can be performed using measurements related to local adhesion, elastic, and electrostatic properties. A Witec pulsed force module coupled to a TA Instruments 2990 Micro-Thermal Analyzer was used with a Thermo-microscope Explorer AFM. A Tektronix TDS 210 oscilloscope was used to monitor the modulated force vs time and to set up the experimental parameters. A series of high-resolution scans were performed on 5 μm × 5 μm areas of the sample. A Thermo-microscopes silicon cantilever probe with a resonant frequency of 23−38 kHz and a tip radius of 10 nm was used. The modulation frequency was set at 500 Hz and the amplitude at 5% of maximum. The indentation force signal used was set to 5 nA.

Results and Discussion

^{29}Si Solid-State CP/MAS NMR. Study by ^{29}Si solid-state NMR was conducted to confirm the cross-linking

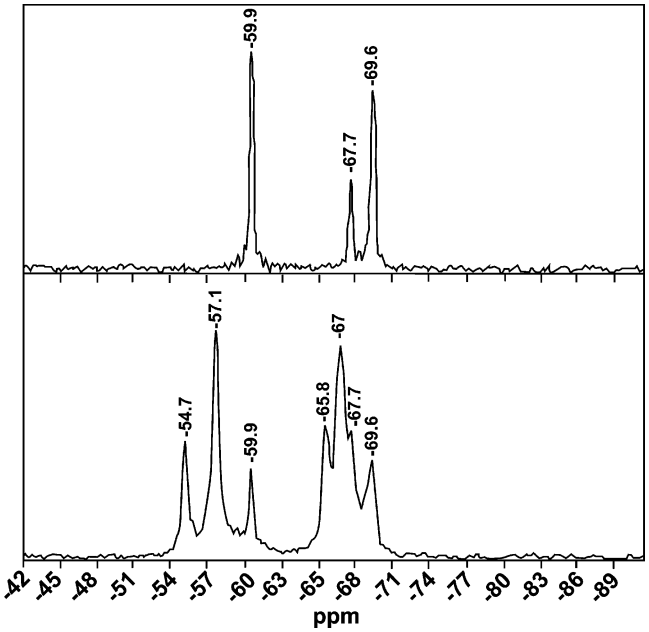

Figure 1. Solid-state ^{29}Si NMR spectra of the pure T-POSS (top) and the T-POSS-urethane hybrid (bottom).

of silicon atoms in the partially cured material. Figure 1 shows the expanded ^{29}Si NMR spectra of pure trisilanol isobutyl T-POSS (top) and the urethane hybrid (bottom).

The pure T-POSS shows three characteristic silicon resonance peaks at −59.9, −67.7, and −69.6 ppm, corresponding to the isobutyl substituted T^2 and T^3 type silicon atoms within the structure. The T^2 resonance peak at −59.9 ppm is assigned to the silicon atoms functionalized with hydroxyl groups, which are connected to two siloxane (−O−Si−) bonds each. Various studies in the literature[21−25] have reported Si−OH groups from POSS molecules to be in the region −57 to −61 ppm. The most pertinent of these studies[21] reported specifically on the chemical shift of a trisilanol POSS molecule ($T_7(OH)_3$) and gave the value of the T^2 silicon atoms at −60.16 ppm, very close to the value noted for this spectra.

The remaining four T^3 silicon atoms in the POSS molecule produce two resonance bands due to the different proximity of one of the T^3 silicon atoms to the T^2 hydroxyl groups. The silicon atom responsible for the extra resonance peak is the silicon atom farthest away from the opening in the cage structure (i.e., the "missing" corner of the POSS cube). Its different proximity to the opening creates differing amounts of ring strain on the silicon atoms within the cage and therefore explains the chemical shift difference between the two types of T^3 silicon atoms present. Silicon atoms present in strained triangular (T_3) cycles have been reported to show resonance bands in the region −54 to −58 ppm.[26,27] These silicon atoms experience more deshielding than silicon atoms in T_8 POSS structures (i.e., having eight silicon atoms in the structure), which have had resonance bands reported in the region −65 to −67 ppm.[28] Thus, silicon atoms in a T_7 type structure (as is the case here) can be expected to fall between the ranges reported for T_3 and T_8 types. Therefore, silicon atoms in polyhedral structures that experience more deshielding than adjacent silicon atoms within the same structure will give rise to separate resonance bands (due to the ring strain), and the bands belonging to the more deshielded silicon atoms will experience a positive chemical shift.[29] Thus, the more positive T^3 resonance band at −67.7 ppm is the silicon atom within the POSS molecule that undergoes the most deshielding (ring strain), which is therefore the silicon atom farthest away from the Si−OH groups.

The spectrum from the T-POSS hybrid shows the appearance of four new silicon resonance bands (compared to the pure POSS) at −54.7, −57.1, −65.8, and −67.0 ppm. It can be seen from the spectra that the resonance bands from the T-POSS monomer are all present, indicating that the T-POSS open cage has remained intact during the formation of the hybrid. The area ratios of the pure T-POSS T^2:T^3 and the two pure T-POSS T^3 bands together, as compared to the raw T-POSS monomer, are different, however. This can be attributed to the formation of urethane linkages and Si−O−Si condensation linkages through the free silanol groups. This also suggests that some T-POSS molecules within the hybrid may not be directly incorporated into the urethane chains and are thus functioning as independent cross-linking agents within the structure.

The molar ratios utilized for the hybrid reaction dictate that the end product will be hydroxyl terminated, as seen from the persistence of the T^2 band (from the raw T-POSS) in the hybrid. The bands at −54.7 and −57.1 ppm (typically within the T^2 range[30,31]) indicate the presence of two new T^2 type silicon atoms. The urethane linkage connected to a silicon atom will form a new T^2 type silicon, but the condensation reaction will of course produce a T^3 silicon.

^{29}Si chemical shifts are highly sensitive to variation in magnetic fields around silicon nuclei, and as such, a condensation reaction between two or more hydroxyl groups from adjacent T-POSS groups will change the magnetic environment of the silicon atoms. This increase in ring strain would cause a positive chemical shift and could thus be responsible for an intense T^3 band in the usual T^2 region. Matejka et al.[29] reported on the self-organization of trialkoxysilanes. This study reported the presence of a possible T^3 silicon at −56.3 ppm due to highly strained three-membered rings. Therefore, it seems reasonable to assign the band at −54.7 ppm to a T^2 silicon arising from deshielding due to the urethane linkage and the band at −57.1 ppm to a T^3 highly strained silicon arising from condensation reactions between T-POSS groups. It is possible that this highly strained T^3 comes from the condensation between hydroxyls on the same T-POSS unit. This type of condensation would produce a very highly strained Si−O−Si linkage. The peaks present at −65.8 and −67.0 ppm are also assigned as T^3 bands (though less strained), resulting from further urethane condensation reactions.

Therefore, the ^{29}Si NMR data suggest that the resulting T-POSS−HDI polyurethane forms a 3D network that consists of polymer chains that are cross-linked through urethane bridges and through the condensation of free silanol groups from T-POSS units within the chains.

Small-Angle Neutron Scattering of the T-POSS−Urethane Hybrid. To examine the growth of the hybrid structure during its formation from solution, a preliminary SANS study was carried out. Stoichiometric amounts of the reactants were dissolved in deuterated toluene; the reaction mixture was then transferred to a SANS cell so that the evolution of the hybrid structure with increasing reaction time could be followed. Because

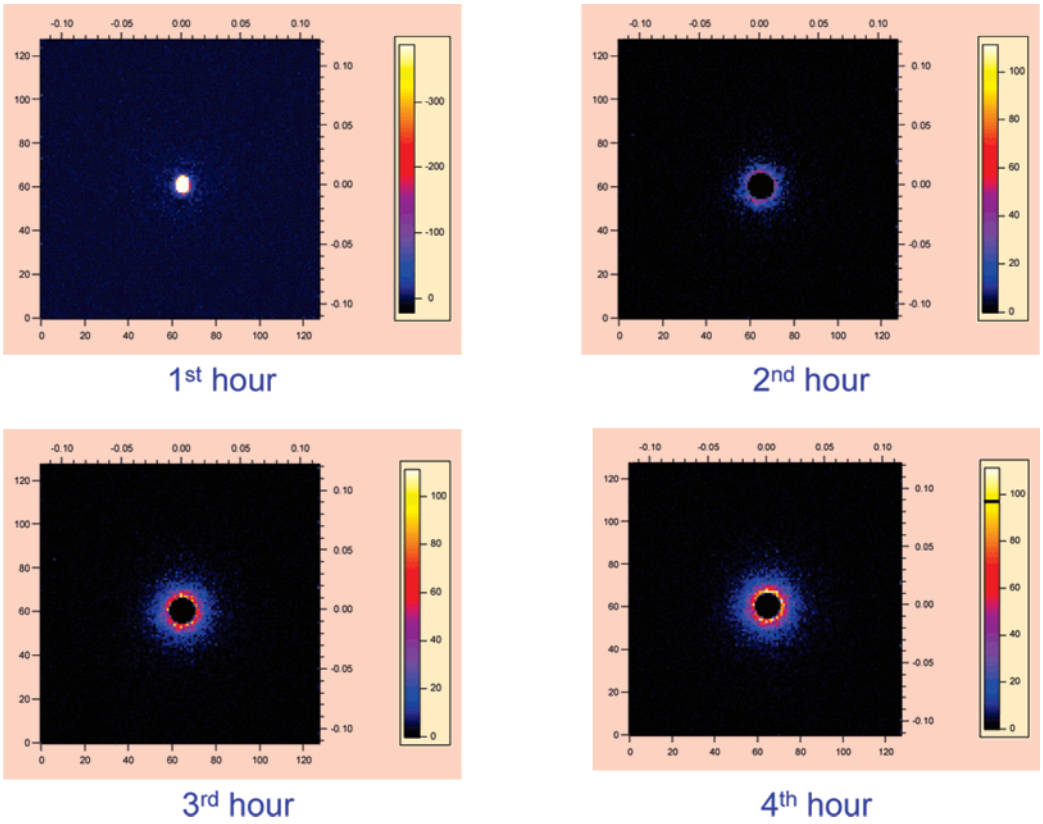

Figure 2. SANS images showing growth of the urethane hybrid at different time periods.

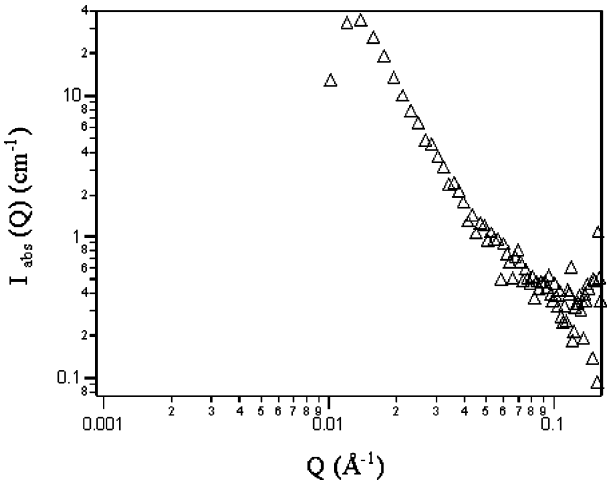

Figure 3. Summed scattered intensity as a function of scattering vector over 4 h reaction time for formation of the T-POSS−urethane hybrid.

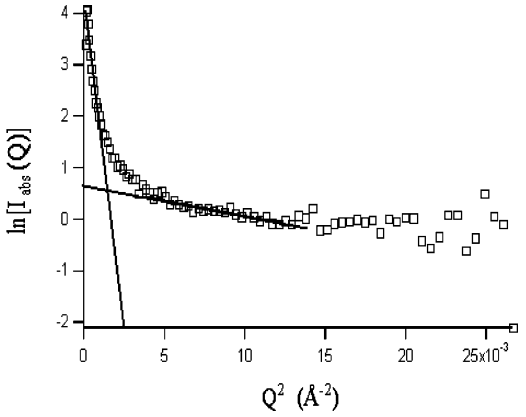

Figure 4. Guinier plots of the low- and high-Q regions.

of the experimental limitations, it was not possible to collect data in the low-Q region to perform an analysis of any low-Q scattering features. The Q range of the instrument (0.01−0.1) would thus only allow for analysis of higher Q data. A more comprehensive SANS study of this and other T-POSS hybrid systems will be reported in our future publication. Figure 2 shows the SANS images collected during the evolution of the T-POSS−urethane hybrid structure at different times of in-situ reaction. Neutron scattering data accumulated at various time periods throughout the 4 h analysis were averaged in Figure 3.

The scattering data show a distinct shift to smaller Q with increasing reaction time. The small Q shift is a result of increasing molecular weight and domain size growth of the hybrid. It can be seen that the scattering curve shows a roughly linear ascent from the high to the low Q limit, whereupon a maximum begins to develop in the scattering ($Q = 0.015$ Å^{-1}). The emergence of this feature at the low Q limit indicates the occurrence of larger aggregates in the hybrid system[32,33] The aggregation behavior is thought to be due to strong interaction between chains as the level of hydrogen bonding, from the amide groups of the urethane chains, increases.

A Guinier plot (Figure 4) of the SANS data from the hybrid shows two regions that display a linear relationship between $\ln[I(Q)]$ and Q^2. This indicates that a Guinier analysis is valid and that the radius of gyration (R_g) may be attained for both regions, provided that the data are analyzed over a Q range in which the QR_g value is close to unity.[34−36] The value of R_g calculated from the Guinier approximation of the higher Q region ($0.064 \leq Q \leq 0.114$ Å^{-1}), where single molecule features give rise to scattering,[33] is ≈14 Å. The Guinier analysis

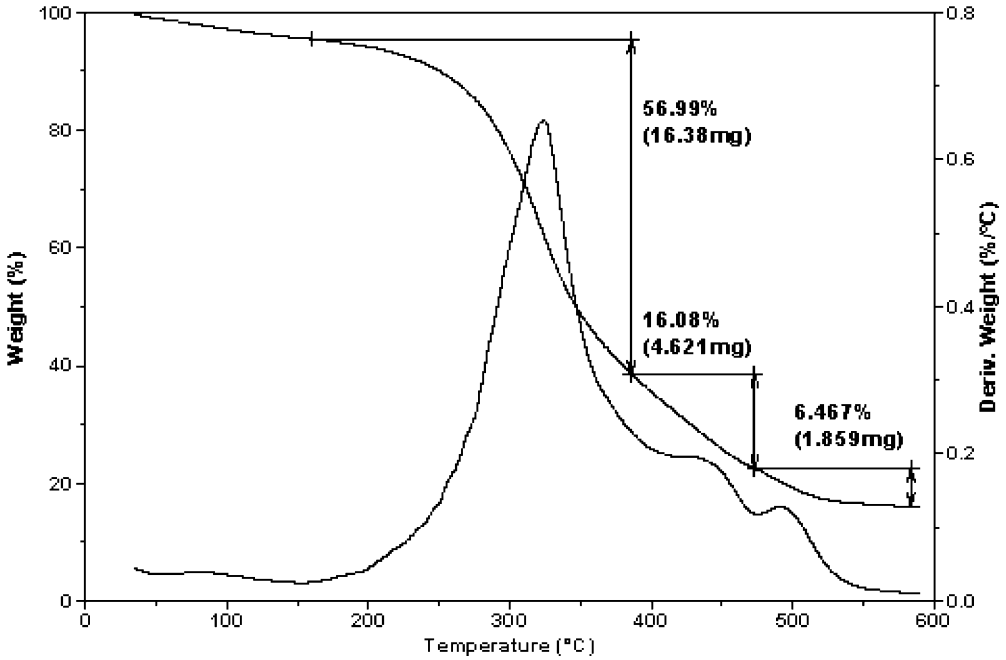

Figure 5. Thermal degradation of T-POSS−urethane by TGA.

of the lower Q region ($0.016 \leq Q \leq 0.025$ Å^{-1}) from the scattering of molecular aggregates suggests that hybrid clusters of $R_g \sim 100$ Å are present.

The trial and application of various models were also examined with the collected data. It is found that a smeared ellipsoid-form particle model best fit the scattering inherent to this system. Manipulation of the fitted variables for this model (scale, rotation axis in a and b directions, R_a and R_b, contrast, and incoherent background), while holding scale (set to particle volume fraction) and incoherent background (known) at known values, shows the ellipsoid to be that of an oblate or disklike form (as $R_b > R_a$). The calculated values of R_a and R_b were ∼35 Å and ∼221 Å, respectively. The marginal deviation obtained from the fitted model suggests that the polymer aggregates formed are closely packed together.

Thermal Stability of the Hybrid. Analysis of the partially cured T-POSS−urethane hybrid using nonisothermal TGA was performed to determine the thermal decomposition temperature of the hybrid. It can be seen in Figure 5 that the degradation of the cured T-POSS−urethane occurs in three stages. Initial mass loss is recorded due to the evaporation of residual solvent. The degradation of the hybrid starts at about 200 °C with a broad mass loss of 56.9% that accounts for both the cleavage of the isobutyl arms and also the cleavage of the weaker urethane linkages. Theoretical calculations based on the reaction stoichiometry show the mass percent of these two components to be around 56% for one repeating unit within a chain. This major mass loss is followed by another mass loss with an onset of about 415 °C (16%) and a third loss at about 470 °C (6.5%). With the organic components of the urethane already degraded, it is apparent that these two peaks can be attributed to the break down of the core Si−O structures of free, partially condensed and completely condensed T-POSS within the remaining residue (20%).

MDSC and PA-FTIR Analysis. MDSC was used to study the reaction and cure kinetics of the hybrid polymer. The decomposition profile was also analyzed. The details of the kinetics analysis will be presented in a separate paper. Stoichiometric amounts of the reactants and catalyst were measured and dissolved in a minimum volume of solvent. A single drop of the concentrated reaction solution was transferred into a hermetic pan for MDSC study. The majority of the solvent was evaporated under a stream of nitrogen, leaving the reactants. This evaporation method was repeated until a reaction mass of ≈8 mg was attained. The time taken for the evaporation process to complete was approximately an hour. Repeated experiments utilizing this method showed that the small amount of solvent remaining in the pan was not sufficient to mask the experiment data. The heat flow signal for the T-POSS-urethane reaction is shown in Figure 6.

It can be seen from the plot that five distinct thermal events (not including the glass transition at 205 °C) occurred from 30 to 550 °C. It is well-known that the condensation reaction of isocyanates and polyol molecules is exothermic. Therefore, the first exothermic peak is assigned as the reaction peak. Identification of other four peaks (all endothermic) was carried out using the unique capabilities of PA-FTIR spectroscopy. IR spectra of the pan residues were recorded at various stages after each thermal event had occurred in order to identify the peaks.

Figures 7a,b show a stack plot and 3D overlay graph showing the initial spectrum, which was taken from a sample pan prior to the subjected heating ramp, and four spectra recorded from pan residues after the first four thermal events. Spectra of the pan residue after the last peak at ≈525 °C could not be obtained due to insufficient signal intensity. To avoid crowding, only the most pertinent bands are labeled in Figure 7a.

The first IR spectrum (the rear-most spectrum in Figure 7b) was taken from a sample pan prior to being subjected to the heating ramp. The main bands are as follows: the band at 2268 cm^{-1}, which is characteristic of isocyanate band −NCO. Next to the isocyanate band is the characteristic double band of carbon dioxide at 2340 and 2365 cm^{-1}; this band appears due to the evaporation method utilized for the analysis. As the solvent is evaporated away, the remaining solvent and

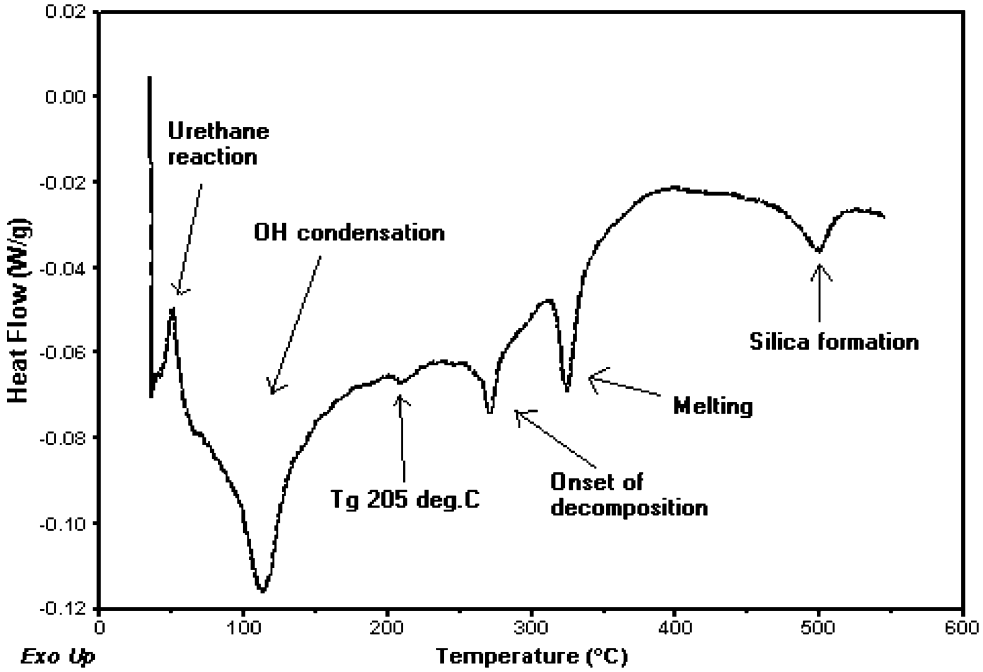

Figure 6. MDSC heat flow signal of T-POSS−urethane formation and decomposition.

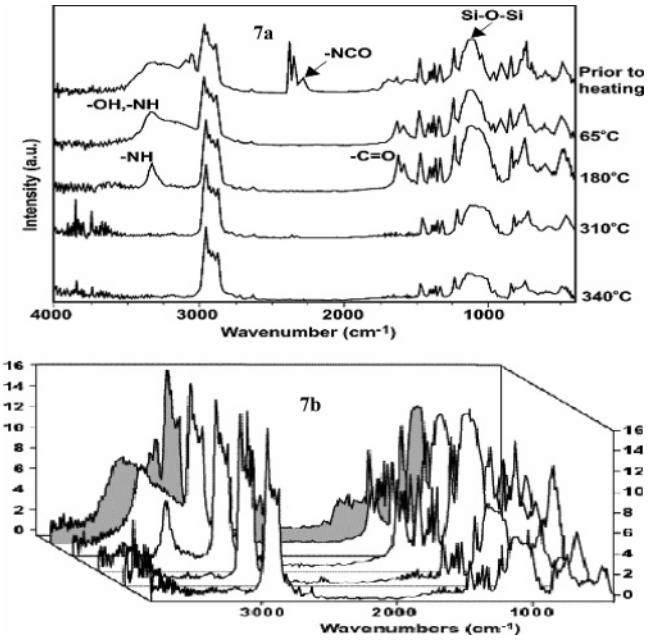

Figure 7. PA-FTIR of reactants after solvent evaporation (partial reaction), IR of residue after first peak in DSC at 65 °C (urethane reaction), IR of residue after second DSC peak at 180 °C (condensation), and IR of residue after third DSC peak at 310 °C (decomposition of urethane linkages) and after fourth peak at 340 °C.

reactants semisolidified, entrapping some carbon dioxide. The two bands present at 3040 and 3080 cm^{-1} are due to the unsaturated hydrocarbon ring from the remaining toluene. Bands due to saturated hydrocarbons originating from the isobutyl group and hexamethylene unit in the hybrid are seen ranging from 2870 to 2960 cm^{-1}. There are several main bands of note (Figure 7a) that are due to the T-POSS. The broad band in the region of 1080−1130 cm^{-1} is characteristic of strong asymmetric Si−O−Si stretching in the T-POSS cage. In the same region are observed bands at 1029 cm^{-1} (Si−butyl) and 907 cm^{-1} (Si−OH). Silsesquioxane skeletal deformation band is present at 580 cm^{-1}. An absorption band of Si−OH is also seen at 3200 cm^{-1}. Because of the evaporation process, which brings reactants into intimate contact, by the time that the solvent is removed and an IR spectrum recorded, some of the reactants have formed a small amount of urethane product. The product bands are observed at 1579 cm^{-1}, which is the amide (−NH) bending vibration of the urethane group and the band at 1621 cm^{-1} due to the urethane carbonyl (C=O). The stretching band of the urethane amide can also be seen at 3329 cm^{-1}.

The second spectrum was taken from the DSC run at which the temperature ramp was stopped at 65 °C. At this temperature the exotherm event had ceased. Several obvious differences from the first spectra are evident. The absence of toluene can be clearly seen from the disappearance of bands at 3040−3080 cm^{-1}. The isocyanate band at 2268 cm^{-1} has completely disappeared along with the decreasing intensity of the Si−OH bands at 907 and 3200 cm^{-1}. The urethane carbonyl band at 1621 cm^{-1} has increased in intensity, as have the bending and stretching bands of the urethane amide at 1579 and 3329 cm^{-1}, respectively. These observations confirm that the first thermal event is indeed that of the exothermic addition reaction between isocyanate and hydroxyl precursors to form the urethane product.

The next DSC run was stopped at 180 °C, at which point the first endothermic event had ceased. It can be seen from the spectra of the pan residue that the Si−OH absorption bands at 907 and 3200 cm^{-1} have completely disappeared. Absence of this band clearly occurs due to the condensation of the remaining hydroxyl groups. This is also apparent due to the broadening of the Si−O−Si band at 1080−1130 cm^{-1} from the addition of a large shoulder at 1065 cm^{-1}. This shoulder is due to the linking of T-POSS molecules through the excess hydroxyl groups. This is further evidenced by the appearance of a broad band at 3600 cm^{-1}, which is likely to be free water—the result of hydroxyl group condensation. The first endothermic peak is thus due to the formation of a three-dimensional urethane network. The amide stretching band of the urethane at 3329 cm^{-1} is

Scheme 1. Proposed Thermal Decomposition Mechanism of the Hybrid

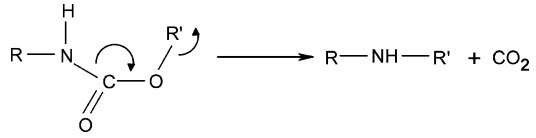

sharp and narrow. This is indicative of decreased hydrogen bonding within the urethane as the remaining hydroxyl groups from the T-POSS molecules condense and continue to form a three-dimensional network.

The next DSC run was stopped at 310 °C after the second endothermic event. As is clearly evident, all of the bands associated with the amide and carbonyl vibrations are no longer present. The band at 1029 cm^{-1} from the isobutyl arms is also no longer present. This event, therefore, represents the thermal degradation of the T-POSS−urethane hybrid via cleavage of the urethane linkages and also cleavage of the isobutyl groups. A small doublet due to carbon dioxide also appeared in the spectra. As the photoacoustic cell undergoes purging with helium gas prior to the spectra being recorded, the carbon dioxide is not due to atmospheric contamination and is, therefore, trapped within the residue; thus, it is a result of the degradation process. At 3200 cm^{-1}, another small band has appeared which is possibly from the formation of an oligomeric primary or secondary amine following the degradation.

The spectrum, taken after the third endothermic event at 340 °C had ceased, did not change at all from the previous event and is, therefore, most likely due to a change of physical state of the T-POSS rather than a change in the chemical structure. A DSC and a TGA were also performed on the pure T-POSS sample, which show the melting of the crystal in the same region without any mass loss. This thermal event thus clearly relates to the melting of crystalline T-POSS present in the sample.

The residue of the DSC pan, taken after the last thermal event, could not produce a strong enough signal for an IR scan to be taken. Only one peak is observed. This peak is most likely due to the formation of silica as the remaining organic species are vaporized. It is not a thermal event such as melting or crystallization, as the TGA data at this temperature show a definite mass loss. It must be pointed out that the TGA was performed on a sample prepared ex-situ under isothermal conditions, while the DSC was performed on an in-situ prepared sample under nonisothermal conditions. TGA results show a mass loss starting at 417 °C that does not appear on the DSC trace. The reason for this mass loss was attributed to the breakdown of free or partially condensed T-POSS units in the hybrid structure. It does not appear in the DSC trace as the IR results clearly show that the hybrid within the pan (prepared nonisothermally) has undergone complete condensation.

Thus, DSC in conjunction with PA-FTIR clearly reveals that the hybrid, upon exposure to high temperatures, is capable of forming a ceramic-passivating layer of silica, which can prevent further degradation of the substrate, thus making it highly suitable for thin film coating application.

The hybrid shows a single glass transition at 205 °C. To confirm this, a second experiment was run under the same conditions, but stopping the temperature ramp at 250 °C before the onset of thermal degradation. As expected, the reaction peak and curing peak occurred

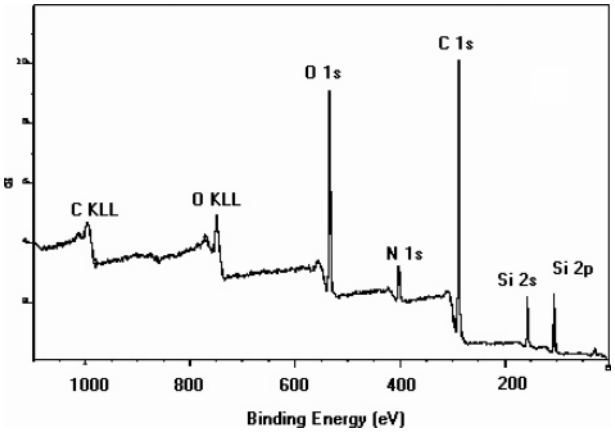

Figure 8. XPS survey spectrum of the hybrid thin film on steel.

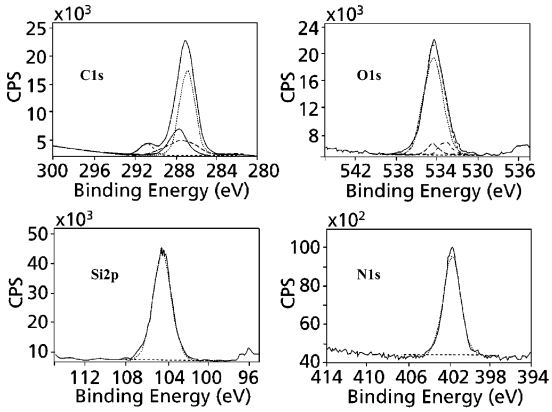

Figure 9. C 1s, O 1s, Si 2p, and N 1s spectra for the hybrid film on metal.

as before, followed by the glass transition at 205 °C. The system was then allowed to cool to ambient temperature, and the same temperature ramp was again applied. On the second run, the only thermal event that occurred was the glass transition at 205 °C. The reaction and curing events completed during the first run were no longer present.

With the information acquired from the TGA and DSC experiments, it is possible to propose the degradation mechanism for the T-POSS−urethane. A review of relevant literature[37−39] shows that polyurethanes are generally thought to thermally decompose via three independent pathways. The first pathway results from the depolymerization of the urethane, back to the original hydroxyl and isocyanate species. The second involves the formation of carbon dioxide and a secondary amine, and the third is due to the formation of carbon dioxide, a primary amine, and an alkene attached to the (former) hydroxyl component.

The IR spectra taken after thermal degradation show no evidence of the first pathway. No bands associated with hydroxyl or isocyanate species are present. The third pathway involves the formation of an alkene species. Bands indicative of unsaturated carbon species do not appear. Carbon dioxide, however, does appear, as does a band that could possibly be due to a primary amine. Therefore, it is the second path (Scheme 1) mentioned above that best fits the observed experimental evidence.

Cyclic DSC. An important property of any thin film coating material is the ability to withstand continued

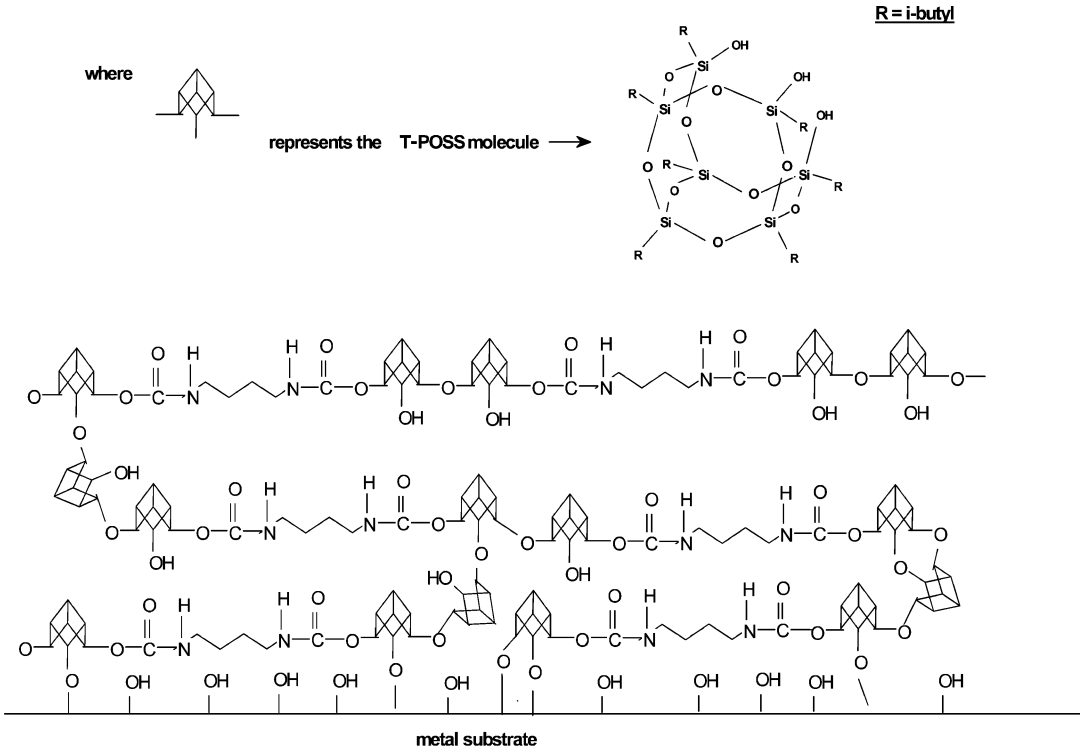

Figure 10. Proposed structure of the hybrid thin film on steel.

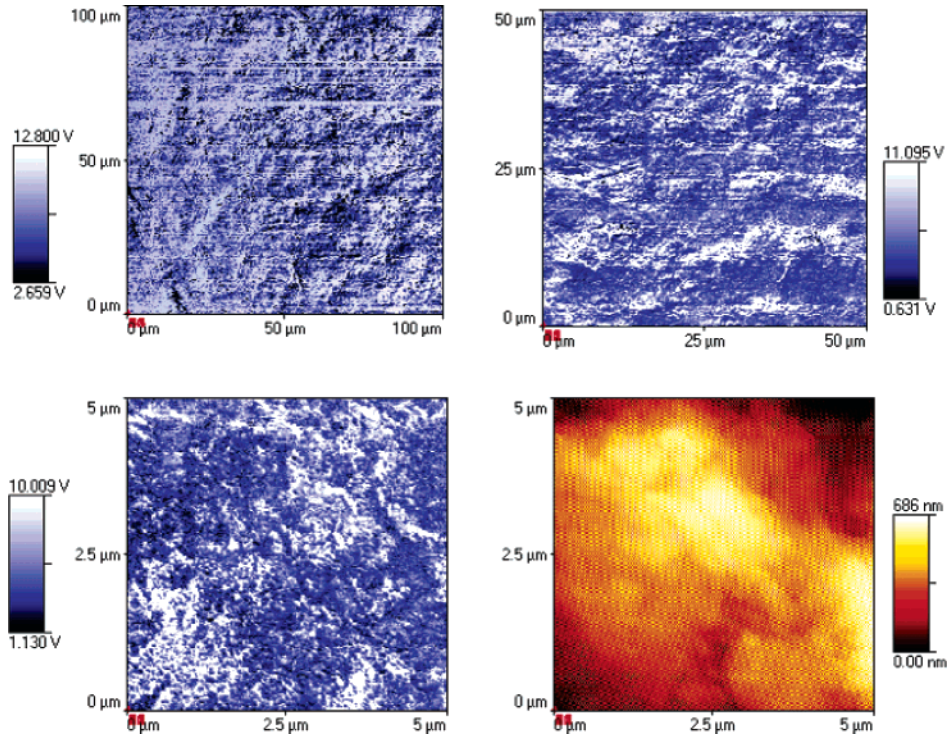

Figure 11. Pull-off force images (100, 50, and 5 μm) and the topography of the hybrid film on steel.

exposure to extremes of temperature while retaining its chemical and structural integrity, provided that the decomposition temperature is not exceeded. To investigate the thermal performance under cyclic conditions, the T-POSS–urethane was subjected to a cyclic temperature test in the DSC. The curing of the hybrid can be seen only at a peak temperature of 123 °C. The hybrid showed no sign of chemical change while being exposed to the temperature extremes on repeated thermal cycling. In general, such thermal cycling also provides information on brittleness and delamination of the coating from the substrate, which occurs due to differential coefficients of thermal expansion. The coated samples were subjected to similar cyclic conditions, and their integrity was examined by pulse force AFM. These results will be presented in a future paper.

Angle-Resolved AR-XPS. The structure of the hybrid coated onto a steel substrate was investigated by AR-XPS. Figure 8 shows a typical XPS survey spectrum of the thin film coating on steel substrate.

Multiplexed spectra were obtained for carbon, oxygen, silicon, and nitrogen. The C 1s major peak, shown in

Table 1. Depth Profile Elemental Concentration Data of Coating

	AR-XPS takeoff angle (deg)				
element	15	30	45	60	90
carbon	65.9	64.1	61.9	61.7	63.9
oxygen	19.2	20.6	21.3	21.5	19.7
silicon	12.2	12.1	13.3	13.6	12.8
nitrogen	1.5	1.7	1.8	1.3	1.8
iron	1.2	1.5	1.7	1.9	1.8

Figure 9, is broad and centered at 284 eV (with charge correction) with a satellite peak at 288 eV. The major peak indicates the presence of aliphatic carbon atoms from the hexamethylene groups in the hybrid and also from the isobutyl groups of the T-POSS open cage. The oxygen atoms present in the urethane that are chemically bonded to carbon are detected as a higher binding energy shoulder to the main peak and are attributed to the C−O, C═O of the urethane. The O 1s spectrum is shown in Figure 9. The predominant forms of oxygen present in the sample correspond to the carbonyl of the urethane group and the oxygen present in the T-POSS cages (533 eV). The Si 2p peak is shown in Figure 9. The peak is broad, indicating the presence of different chemical states of silicon. The peak is centered at 102.7 eV, which corresponds to the RSiOn in the T-POSS open cage. Similar results for the Si 2p binding energy have been observed for polymeric networks containing Si−O−Si linkages.[40,41] The major N 1s peak (Figure 9) occurs at 399.8 eV, which corresponds to the amide group of the urethane.

The elemental compositions of the T-POSS−urethane coating determined at different takeoff angles are presented in Table 1. As can be seen in the table, the elements comprising the T-POSS−urethane are all present and in approximately the correct ratios as calculated from the stoichiometry. Iron from the steel substrate also registers, indicating the coating depth to be 7 nm or less—the accepted sensitivity of this technique. Thus, we can determine the assembly of the coating at the metal coating interface as well as the bulk coating structure. Other analyses of this system that we have conducted using more concentrated dipping solutions (2−5% m/v) have yielded coatings too thick for the substrate to be seen.

The elemental concentration data show marginal differences in the atomic concentration of each element at different depths, indicating the formation of a lamellar network structure of T-POSS−urethane rather than a specific orientation due to a preferential functional group−substrate interaction. Figure 10 shows a schematic of the T-POSS−urethane bulk and interface structure, as evidenced by the AR-XPS data. The long-range ordered lamellar structure of the hybrid results from the strong hydrogen-bonding interactions of the amide groups in the urethanes and the long-range hydrophobic interactions of the hexamethylene and isobutyl groups.

Pulsed Force Microscopy. Figure 11 shows 100 and 50 μm pull-off force images (top) and 5 μm × 5 μm pull-off force image and topography (bottom) from the urethane−T-POSS hybrid on metal. To check whether topography is responsible for spatial variations in pull-off force for a particular sample, the respective distributions of the two measurements were compared. No phase-separated morphology was evident, indicating that the hybrid is a homogeneous one-phase material. The negative enthalpy obtained from the covalent reaction and attachment of silanol and the isocyanate groups leads to such a fine level of dispersion.

Conclusions

We have successfully synthesized a new class of hybrid polyurethane that is suitable for coating applications. Upon curing, the hybrid forms a 3D network with a high degree of cross-linking, which makes the hybrid ideal for selection as a barrier coating for the protection of metals substrates. Importantly, the T-POSS components retain their partial cage structure, which give the product a high glass transition and high thermal stability as compared to conventional polyurethanes, which is essential in their application as weatherable coatings. This was further shown when upon repeated exposure to high and low temperatures the hybrid retained its chemical and structural integrity. The application of the hybrid as a coating resulted in the formation of a homogeneous one-phase lamellar coating with excellent coverage of the substrate.

Acknowledgment. We gratefully acknowledge the financial support of Australian Institute of Science and Nuclear Engineering, AINSE, Australian Research Council's Special Research Centre, ARC−SRC, and especially Dr. Robert Knott of ANSTO for his assistance in carrying out the SANS measurements and Dr. Andrew Whittaker of Centre for Magnetic Resonance, University of Queensland, for carrying out the ^{29} Si NMR work.

References and Notes

(1) Sugama, T. *Mater. Lett.* **1995**, *25*, 291.
(2) Choi, J.; Yee, A. F.; Laine, R. M. *Macromolecules* **2004**, *37*, 3267.
(3) Lee, A.; Lichtenhan, J. D. *Macromolecules* **1998**, *31*, 4970.
(4) Zheng, L.; Hong, S.; Cardoen, G.; Burgaz, E.; Gido, S. P.; Coughlin, E. B. *Macromolecules* **2004**, *37*, 8606.
(5) Wright, M. E.; Schorzman, D. A.; Feher, F. J.; Jin, R. Z. *Chem. Mater.* **2003**, *15*, 264.
(6) Choi, J.; Kim. S. G.; Laine, R. M. *Macromolecules* **2004**, *37*, 99.
(7) Mather, P. T.; Jeon, H. G.; Romo-Ubride, A.; Haddad, T. S.; Lichtenhan, J. D. *Macromolecules* **1999**, *32*, 1194.
(8) Bharadwaj, R. K.; Berry, R. J.; Farmer, B. L. *Polymer* **2000**, *41*, 7209.
(9) Neumann, D.; Fisher, M.; Tran, L.; Matisons, J. G. *J. Am. Chem. Soc.* **2002**, *124*, 13, 998.
(10) Fu, B. X.; Hsiao, B. S.; White, H.; Rafailovich, M. P.; White, H.; Mather, P. T.; Jeon, H. G.; Phillips, S.; Lichtenhan, J.; Schwab, J. *Polym. Int.* **2000**, *49*, 437.
(11) Hsiao, B. S.; Fu, B. X.; Pagola, S.; Stephens, P.; White, H.; Rafailovich, M.; Sokolov, J.; Mather, P. T.; Jeon, H. G.; Phillips, S.; Lichtenhan, J.; Schwab, J. *Polymer* **2001**, *42*, 599.
(12) Wilkes, G. L.; Li, C. *Polym. Prepr.* **1999**, *40*, 778.
(13) Galliano, P.; De Damborenea, J. J.; Pascual, M. J.; Duran, A. *J. Sol-Gel Sci. Technol.* **1998**, *13*, 723.
(14) Van Ooij, W. J.; Yuan, W. *J. Colloid Interface Sci.* **1997**, *185*, 197.
(15) Van Ooij, W. J.; Song, J. *ATB Metall.* **1997**, *37*, 137.
(16) Puomi, P.; Fagerholm, H. K. *J. Adhes. Sci. Technol.* **2001**, *15*, 869.
(17) Plueddemann, E. P. *Silane Coupling Agents*, 2nd ed.; Plenum: New York, 1991.
(18) Brook, M. A. *Silicon in Organic, Organometallic and Polymer Chemistry*; Wiley-Interscience: New York, 2000.
(19) Miyatani, T.; Horri, M.; Rosa-Zeiser, A.; Fujihara, M.; Marti, O. *Appl. Phys. Lett.* **1997**, *71*, 2632.
(20) Gao, Y.; Roy Choudhury, N.; Dutta, N.; Matisons, J.; Reading, M.; Delmotte, D. *Chem. Mater.* **2001**, *13*, 3644.
(21) Feher, F. J.; Newman, D. A.; Walzer, J. F. *J. Am. Chem. Soc.* **1989**, *111*, 1741.
(22) Feher, F. J.; Budzichowski, T. A.; Blanski, R. L.; Weller, K. J.; Ziller, J. W. *Organometallics* **1991**, *10*, 2526.
(23) Feher, F. J.; Souvilong, D.; Eklund, A. G. *Chem. Commun.* **1998**, 399.

(24) Feher, F. J.; Souvilong, D.; Nguyen, F. *Chem. Commun.* **1998**, 1279.
(25) Fasce, D. P.; Williams, R. J. J.; Mechin, F.; Pascault, J. P.; Llauro, M. F.; Petiaud, R. *Macromolecules* **1999**, *32*, 4757.
(26) Unno, M.; Alias, S. B.; Saito, H.; Matsumoto, H. *Organometallics* **1996**, *15*, 2413.
(27) Feher, F. J.; Souvilong, D.; Lewis, G. T. *J. Am. Chem. Soc.* **1997**, *119*, 11323.
(28) Rikowski, E.; Marsmann, H. C. *Polyhedron* **1997**, *16*, 3357.
(29) Matejka, L.; Dukh, O.; Hlavata, D.; Meissner, B.; Brus, J. *Macromolecules* **2001**, *34*, 6904.
(30) Schneider, M.; Mullen, K. *Chem. Mater.* **2000**, *12*, 352.
(31) Innocenzi, P.; Brusatin, G.; Licoccia, S.; Di Vona, M. L.; Babonneau, F.; Alonso, B. *Chem. Mater.* **2003**, *15*, 4790.
(32) Edelmann, K.; Janich, M.; Hoinkis, E.; Pyckhout-Hintzen, W.; Horing, S. *Macromol. Chem. Phys.* **2001**, *202*, 1638.
(33) Beck Tan, N. C.; Balogh, L.; Trevino, S. F.; Tomalia, D. A.; Lin, J. S. *Polymer* **1999**, *40*, 2537.
(34) Guinier, A.; Fournet, G. *Small Angle Scattering of X-Rays*; Wiley: New York, 1955.
(35) Richards, R. W.; Thomason, J. L. *Polymer* **1981**, *22*, 581.
(36) Bates, F. S.; Berney, C. V.; Cohen, R. E.; Wignall, G. D. *Polymer* **1983**, *25*, 519.
(37) Dyer, E.; Newborn, G. E. *J. Am. Chem. Soc.* **1958**, *80*, 5495.
(38) Dyer, E.; Reed, R. E. *J. Org. Chem.* **1961**, *26*, 4388.
(39) Grassie, N.; Scott, G. *Polymer Degradation and Stabilisation*; Cambridge University Press: New York, 1985.
(40) Wagner, C. D.; Passoja, D. E.; Hillery, H. F.; Kinisky, T. G.; Six, H. A.; Jansen, W. T.; Taylor, J. A. *J. Vac. Sci. Technol.* **1982**, *21*, 933.
(41) Leung, Y. L.; Zhou, M. Y.; Wong, P. C.; Mitchell, K. A. R. *Appl. Surf. Sci.* **1992**, *59*, 23.

MA0476543